

# Dynamics of Entanglement and Uncertainty Relation in Coupled Harmonic Oscillator System : Exact Results

DaeKil Park<sup>1,2</sup>

<sup>1</sup>*Department of Electronic Engineering,*

*Kyungnam University, Changwon 631-701, Korea*

<sup>2</sup>*Department of Physics, Kyungnam University, Changwon 631-701, Korea*

## Abstract

The dynamics of entanglement and uncertainty relation is explored by solving the time-dependent Schrödinger equation of the coupled harmonic oscillator system analytically when the angular frequencies and coupling constant are arbitrarily time-dependent. We derive the spectral and Schmidt decompositions for the vacuum solution. Using the decompositions we derive the analytical expressions for von Neumann and Rényi entropies. Making use of Wigner function, we derive also the time-dependence of position-momentum uncertainty relations. To show the dynamics of entanglement and uncertainty relation graphically we introduce two toy models and one realistic quenched model. While the dynamics can be conjectured by simple consideration in the toy models, the dynamics in the realistic quenched model is somewhat different from those in the toy models. In particular, the dynamics of entanglement exhibits similar pattern to dynamics of uncertainty parameter in the realistic quenched model.

## I. INTRODUCTION

Another nickname of quantum entanglement[1–3] is ‘spooky action at a distance’ due to EPR paradox[4]. Although the debate related to EPR paradox does not reach a complete conclusion, many theorists use the entanglement as a physical resource to develop the various quantum information processing such as quantum teleportation[5], superdense coding[6], quantum cloning[7], and quantum cryptography[8, 9]. It is also quantum entanglement, which makes the quantum computer outperform the classical one[10, 11]. Furthermore, many experimentalists tried to realize such quantum information processing in the laboratory for last decade. In particular, quantum cryptography seems to approaching to the commercial level[12].

In addition to the quantum technology quantum entanglement is important notion in various branches of physics. The von Neumann[13] and Rényi entropies[14], which are frequently used to measure the bipartite entanglement, enable us to understand the Hawking-Bekenstein entropy[15–20] of black holes more deeply. They are also important to study on the quantum criticality[21, 22] and topological matters[23, 24].

Another important cornerstone in quantum mechanics is a uncertainty relation[25], which arises due to wave-particle dual property in the isolated systems. In this paper we examine the dynamics of the entanglement and uncertainty relation in coupled harmonic oscillator system, where the angular frequencies and coupling constant are arbitrarily time-dependent. The harmonic oscillator system is used in many branches of physics due to the fact that its mathematical simplicity provides a clear illustration of abstract ideas. For example, the coupled system was used in Ref. [26] to discuss on the effect of the rest of universe[27]. It was shown that ignoring the rest of universe appears as an increase of uncertainty and entropy in the system in which we are interested. The analytical expression of von Neumann entropy was derived for a general real Gaussian density matrix in Ref. [18] and it was generalized to massless scalar field in Ref. [19]. Putting the scalar field system in the spherical box, the author in Ref. [19] has shown that the total entropy of the system is proportional to surface area. This result gives some insight into the question why the Hawking-Bekenstein entropy is proportional to the area of the event horizon. Recently, the entanglement is computed in the coupled harmonic oscillator system using a Schmidt decomposition[28]. The von Neumann and Rényi entropies are also explicitly computed in the similar system, called two

site Bose-Hubbard model[29]. The coupled harmonic oscillator system is also used in other branches such as molecular chemistry[30, 31] and biophysics[32, 33].

This paper is organized as follows. In next section the diagonalization of the Hamiltonian is discussed briefly. In Sec. III we derive the solutions for time-dependent Schrödinger equation (TDSE) explicitly in the coupled harmonic oscillator system. In Sec. IV we derive the spectral and Schmidt decompositions for the vacuum solution. Using the decompositions we derive von Neumann and Rényi entropies analytically if the oscillators are in the ground states initially. In Sec. V we derive a dynamics of position-momentum uncertainty relation by making use of the Wigner function. In Sec. VI we introduce two toy models and one more realistic quenched model and derive the time-dependence of entanglement and uncertainty relation analytically. It is shown that in the quenched model the pattern of uncertainty is similar to that of entanglement. In Sec. VII a conclusion is given. The dynamics in the excited states is briefly discussed in this section.

## II. DIAGONALIZATION OF HAMILTONIAN

Let us consider the following Hamiltonian of coupled harmonic oscillator system

$$H = \frac{1}{2}(p_1^2 + p_2^2) + \frac{1}{2}(\omega_1^2(t)x_1^2 + \omega_2^2(t)x_2^2) - J(t)x_1x_2 \quad (2.1)$$

where  $\{x_i, p_i\}$  ( $i = 1, 2$ ) are the canonical coordinates and momenta, and frequencies  $\omega_j$  ( $j = 1, 2$ ) and coupling parameter  $J$  are arbitrarily dependent on time. For simplicity, we assume that the oscillators have unit masses. Now, we define a rotation angle  $\alpha$  as

$$\begin{pmatrix} y_1 \\ y_2 \end{pmatrix} = \begin{pmatrix} \cos \alpha & -\sin \alpha \\ \sin \alpha & \cos \alpha \end{pmatrix} \begin{pmatrix} x_1 \\ x_2 \end{pmatrix}. \quad (2.2)$$

If we choose  $\alpha$  as

$$\alpha = \frac{1}{2} \tan^{-1} \left( \frac{2J}{\omega_1^2 - \omega_2^2} \right) \quad (2.3)$$

with  $-\pi/4 \leq \alpha \leq \pi/4$ , the Hamiltonian is diagonalized as a form:

$$H = \frac{1}{2}(\tilde{p}_1^2 + \tilde{p}_2^2) + \frac{1}{2}(\tilde{\omega}_1^2(t)y_1^2 + \tilde{\omega}_2^2(t)y_2^2) \quad (2.4)$$

where

$$\begin{aligned} \tilde{\omega}_1^2 &= \omega_1^2 + J \tan \alpha = \frac{1}{2} \left[ (\omega_1^2 + \omega_2^2) + \epsilon(\omega_1^2 - \omega_2^2) \sqrt{(\omega_1^2 - \omega_2^2)^2 + 4J^2} \right] \\ \tilde{\omega}_2^2 &= \omega_2^2 - J \tan \alpha = \frac{1}{2} \left[ (\omega_1^2 + \omega_2^2) - \epsilon(\omega_1^2 - \omega_2^2) \sqrt{(\omega_1^2 - \omega_2^2)^2 + 4J^2} \right] \end{aligned} \quad (2.5)$$

with  $\epsilon(x) = x/|x|$ . Of course,  $\tilde{p}_j = -i\partial/\partial y_j$  ( $j = 1, 2$ ) are canonical momenta of  $y_j$ . In next section we will use the diagonalized Hamiltonian (2.4) to solve the TDSE of the original Hamiltonian (2.1).

### III. SOLUTIONS OF TDSE

Consider a Hamiltonian of single harmonic oscillator with time-dependent frequency

$$H = \frac{p^2}{2} + \frac{1}{2}\omega^2(t)x^2. \quad (3.1)$$

The TDSE of the Hamiltonian was exactly solved in Ref. [34, 35]. The linearly independent solutions  $\psi_n(x, t)$  ( $n = 0, 1, \dots$ ) are expressed in a form

$$\psi_n(x, t) = e^{-iE_n\tau(t)} e^{\frac{i}{2}\left(\frac{\dot{b}}{b}\right)x^2} \phi_n\left(\frac{x}{b}\right) \quad (3.2)$$

where

$$E_n = \left(n + \frac{1}{2}\right) \omega(0) \quad \tau(t) = \int_0^t \frac{ds}{b^2(s)} \quad (3.3)$$

$$\phi_n(x) = \frac{1}{\sqrt{2^n n!}} \left(\frac{\omega(0)}{\pi b^2}\right)^{1/4} H_n\left(\sqrt{\omega(0)}x\right) e^{-\frac{\omega(0)}{2}x^2}.$$

In Eq. (3.3)  $H_n(z)$  is  $n^{\text{th}}$ -order Hermite polynomial and  $b(t)$  satisfies the Ermakov equation

$$\ddot{b} + \omega^2(t)b = \frac{\omega^2(0)}{b^3} \quad (3.4)$$

with  $b(0) = 1$  and  $\dot{b}(0) = 0$ . Solution of the Ermakov equation was discussed in Ref. [36]. If  $\omega(t)$  is time-independent,  $b(t)$  is simply one. If  $\omega(t)$  is instantly changed as

$$\omega(t) = \begin{cases} \omega_i & t = 0 \\ \omega_f & t > 0, \end{cases} \quad (3.5)$$

then  $b(t)$  becomes

$$b(t) = \sqrt{\frac{\omega_f^2 - \omega_i^2}{2\omega_f^2} \cos(2\omega_f t) + \frac{\omega_f^2 + \omega_i^2}{2\omega_f^2}}. \quad (3.6)$$

Recently, the solution (3.6) is extensively used to discuss the entanglement dynamics for the sudden quenched states of two site Bose-Hubbard model in Ref. [29]. Since TDSE is a linear differential equation, the general solution of TDSE is  $\Psi(x, t) = \sum_{n=0}^{\infty} c_n \psi_n(x, t)$  with  $\sum_{n=0}^{\infty} |c_n|^2 = 1$ . The coefficient  $c_n$  is determined by making use of the initial condition.

Using Eqs. (2.4) and (3.2) the general solution for TDSE of the coupled harmonic oscillators are  $\Psi(x_1, x_2 : t) = \sum_n \sum_m c_{n,m} \psi_{n,m}(x_1, x_2 : t)$ , where  $\sum_n \sum_m |c_{n,m}|^2 = 1$  and

$$\begin{aligned} \psi_{n,m}(x_1, x_2 : t) = & \frac{1}{\sqrt{2^{n+m} n! m!}} \left( \frac{\omega'_1 \omega'_2}{\pi^2} \right)^{1/4} \text{Exp} \left[ -i(E_n \tau_1 + E_m \tau_2) \right. \\ & - \frac{\omega'_1}{2} (x_1 \cos \alpha - x_2 \sin \alpha)^2 - \frac{\omega'_2}{2} (x_1 \sin \alpha + x_2 \cos \alpha)^2 \\ & \left. + \frac{i}{2} \left\{ \left( \frac{\dot{b}_1}{b_1} \right) (x_1 \cos \alpha - x_2 \sin \alpha)^2 + \left( \frac{\dot{b}_2}{b_2} \right) (x_1 \sin \alpha + x_2 \cos \alpha)^2 \right\} \right] \\ & \times H_n \left[ \sqrt{\omega'_1} (x_1 \cos \alpha - x_2 \sin \alpha) \right] H_m \left[ \sqrt{\omega'_2} (x_1 \sin \alpha + x_2 \cos \alpha) \right]. \end{aligned} \quad (3.7)$$

In Eq. (3.7)  $b_j$  ( $j = 1, 2$ ) satisfy the Ermakov equations  $\ddot{b}_j + \tilde{\omega}_j^2(t) b_j = \frac{\tilde{\omega}_j^2(0)}{b_j^3}$  respectively, and

$$\tau_j = \int_0^t \frac{ds}{b_j^2(s)} \quad \omega'_j = \frac{\tilde{\omega}_j(0)}{b_j^2}. \quad (3.8)$$

The corresponding density matrix is defined as

$$\rho(x_1, x_2 : x'_1, x'_2 : t) = \Psi(x_1, x_2 : t) \Psi^*(x'_1, x'_2 : t). \quad (3.9)$$

If two oscillators are  $n^{\text{th}}$ – and  $m^{\text{th}}$ –states initially, the density matrix becomes

$$\begin{aligned} \rho_{n,m}(x_1, x_2 : x'_1, x'_2 : t) = & \psi_{n,m}(x_1, x_2 : t) \psi_{n,m}^*(x'_1, x'_2 : t) \\ = & \frac{\sqrt{\omega'_1 \omega'_2}}{2^{n+m} n! m! \pi} H_n \left[ \sqrt{\omega'_1} (x_1 \cos \alpha - x_2 \sin \alpha) \right] H_n \left[ \sqrt{\omega'_1} (x'_1 \cos \alpha - x'_2 \sin \alpha) \right] \\ & \times H_m \left[ \sqrt{\omega'_2} (x_1 \sin \alpha + x_2 \cos \alpha) \right] H_m \left[ \sqrt{\omega'_2} (x'_1 \sin \alpha + x'_2 \cos \alpha) \right] \\ \times \text{Exp} & \left[ -\frac{x_1^2}{2} (v_1 \cos^2 \alpha + v_2 \sin^2 \alpha) - \frac{x_2^2}{2} (v_1 \sin^2 \alpha + v_2 \cos^2 \alpha) + x_1 x_2 \sin \alpha \cos \alpha (v_1 - v_2) \right] \\ \times \text{Exp} & \left[ -\frac{x'_1{}^2}{2} (v_1^* \cos^2 \alpha + v_2^* \sin^2 \alpha) - \frac{x'_2{}^2}{2} (v_1^* \sin^2 \alpha + v_2^* \cos^2 \alpha) + x'_1 x'_2 \sin \alpha \cos \alpha (v_1^* - v_2^*) \right] \end{aligned} \quad (3.10)$$

where  $v_j = \omega'_j - i \frac{\dot{b}_j}{b_j}$ . In next section we will discuss on the entanglement of the vacuum state  $\rho_{0,0}(x_1, x_2 : x'_1, x'_2 : t)$ .

#### IV. ENTANGLEMENT

In order to explore the entanglement of the vacuum states we will derive the Schmidt decomposition of  $\psi_{0,0}(x_1, x_2 : t)$  and the spectral decomposition of the reduced density matrix explicitly. The reduced density matrix of the first oscillator is given by

$$\rho_{(0,0)}^A(x_1, x'_1 : t) \equiv \int dx_2 \rho_{0,0}(x_1, x_2 : x'_1, x_2 : t). \quad (4.1)$$

The explicit expression of the reduced density matrix is

$$\rho_{(0,0)}^A(x_1, x'_1 : t) = \sqrt{\frac{2a_1}{\pi}} \text{Exp} \left[ - \{ (a_1 + a_3) - ia_2 \} x_1^2 - \{ (a_1 + a_3) + ia_2 \} x'_1{}^2 + 2a_3 x_1 x'_1 \right] \quad (4.2)$$

where

$$a_1 = \frac{\omega'_1 \omega'_2}{2D} \quad a_2 = \frac{\omega'_1 \frac{b_2}{b_1} \sin^2 \alpha + \omega'_2 \frac{b_1}{b_2} \cos^2 \alpha}{2D} \quad a_3 = \frac{\sin^2 \alpha \cos^2 \alpha \left[ (\omega'_1 - \omega'_2)^2 + \left( \frac{b_1}{b_1} - \frac{b_2}{b_2} \right)^2 \right]}{4D} \quad (4.3)$$

with  $D = \omega'_1 \sin^2 \alpha + \omega'_2 \cos^2 \alpha$ . One can show easily

$$\text{Tr} [\rho_{(0,0)}^A] \equiv \int dx \rho_{(0,0)}^A(x, x : t) = 1 \quad (4.4)$$

$$\text{Tr} \left[ \left( \rho_{(0,0)}^A \right)^2 \right] \equiv \int dx dx' \rho_{(0,0)}^A(x, x' : t) \rho_{(0,0)}^A(x', x : t) = \sqrt{\frac{a_1}{a_1 + 2a_3}} = \sqrt{\frac{\omega'_1 \omega'_2}{\bar{\eta}}}$$

where  $\bar{\eta} = D\tilde{D} + \sin^2 \alpha \cos^2 \alpha \left( \frac{b_1}{b_1} - \frac{b_2}{b_2} \right)^2$  with  $\tilde{D} = \omega'_1 \cos^2 \alpha + \omega'_2 \sin^2 \alpha$ . First equation of Eq. (4.4) guarantees the probability conservation and second one denotes the mixedness of  $\rho_{(0,0)}^A(x, x' : t)$ . If it is one, this means that  $\rho_{(0,0)}^A(x, x' : t)$  is pure state. On the contrary if it is zero, this means that  $\rho_{(0,0)}^A(x, x' : t)$  is completely mixed state. If  $\tilde{\omega}_j$  are independent of time,  $\omega'_j = \tilde{\omega}_j$  and  $\text{Tr} \left[ \left( \rho_{(0,0)}^A \right)^2 \right]$  becomes  $\sqrt{\omega'_1 \omega'_2 / (D\tilde{D})}$ . Thus, if  $\alpha = 0$ ,  $\rho_{(0,0)}^A(x, x' : t)$  becomes pure state. The most strong mixed state occurs at  $\alpha = \pm\pi/4$ , In this case  $\text{Tr} \left[ \left( \rho_{(0,0)}^A \right)^2 \right]$  becomes  $2\sqrt{\omega'_1 \omega'_2} / (\omega'_1 + \omega'_2)$ .

In order to derive the spectral decomposition of  $\rho_{(0,0)}^A(x, x' : t)$  we should solve the following eigenvalue equation;

$$\int_{-\infty}^{\infty} dx' \rho_{(0,0)}^A(x, x' : t) f_n(x', t) = p_n(t) f_n(x', t). \quad (4.5)$$

Similar problem were discussed in Ref. [18, 19, 29]. It is not difficult to show that the eigenvalue and normalized eigenfunction in this case become

$$f_n(x, t) = \frac{1}{\sqrt{2^n n!}} \left( \frac{\epsilon}{\pi} \right)^{1/4} H_n(\sqrt{\epsilon} x) \text{Exp} \left[ -\frac{\epsilon}{2} x^2 + ia_2 x^2 \right] \quad p_n(t) = (1 - \xi) \xi^n \quad (4.6)$$

where

$$\epsilon = 2\sqrt{(a_1 + a_3)^2 - a_3^2} \quad \xi = \frac{a_3}{(a_1 + a_3) + \frac{\epsilon}{2}}. \quad (4.7)$$

Thus, the spectral decomposition of  $\rho_{(0,0)}^A(x, x' : t)$  can be written as

$$\rho_{(0,0)}^A(x, x' : t) = \sum_{n=0}^{\infty} p_n(t) f_n(x, t) f_n^*(x', t). \quad (4.8)$$

This can be proved explicitly by making use of a mathematical formula

$$\sum_{n=0}^{\infty} \frac{t^n}{n!} H_n(x) H_n(y) = (1 - 4t^2)^{-1/2} \text{Exp} \left[ \frac{4txy - 4t^2(x^2 + y^2)}{1 - 4t^2} \right].$$

Thus Rényi and von Neumann entropies are given by

$$S_n \equiv \frac{1}{1-n} \ln \text{Tr} \left( (\rho_{(0,0)}^A(x, x' : t))^n \right) = \frac{1}{1-n} \ln \frac{(1-\xi)^n}{1-\xi^n} \quad (4.9)$$

$$S_{von} \equiv \lim_{n \rightarrow 1} S_n = -\ln(1-\xi) - \frac{\xi}{1-\xi} \ln \xi$$

where  $n$  is any positive integer. It is worthwhile noting that when  $\alpha = 0$ ,  $\xi$  becomes zero which results in vanishing Rényi and von Neumann entropies. It is obvious because  $\alpha = 0$  corresponds to  $J = 0$  and,  $x_1$  and  $x_2$  are decoupled in the Hamiltonian (2.1).

In order to derive the Schmidt decomposition of  $\psi_{0,0}(x_1, x_2 : t)$  we should solve the eigenvalue equation of other party. The reduced density matrix of other party is given by

$$\rho_{(0,0)}^B(x_2, x'_2 : t) \equiv \int dx_1 \rho_{0,0}(x_1, x_2 : x_1, x'_2 : t) \quad (4.10)$$

$$= \sqrt{\frac{2\tilde{a}_1}{\pi}} \text{Exp} \left[ -\{(\tilde{a}_1 + \tilde{a}_3) - i\tilde{a}_2\} x_2^2 - \{(\tilde{a}_1 + \tilde{a}_3) + i\tilde{a}_2\} x'_2{}^2 + 2\tilde{a}_3 x_2 x'_2 \right]$$

where

$$\tilde{a}_1 = \frac{\omega'_1 \omega'_2}{2\tilde{D}} \quad \tilde{a}_2 = \frac{\omega'_1 \frac{b_2}{b_1} \cos^2 \alpha + \omega'_2 \frac{b_1}{b_2} \sin^2 \alpha}{2\tilde{D}} \quad \tilde{a}_3 = \frac{\sin^2 \alpha \cos^2 \alpha \left[ (\omega'_1 - \omega'_2)^2 + \left( \frac{b_1}{b_1} - \frac{b_2}{b_2} \right)^2 \right]}{4\tilde{D}}. \quad (4.11)$$

The eigenvalues of  $\rho_{(0,0)}^B$  are exactly the same with those of  $\rho_{(0,0)}^A$  and the eigenfunction becomes

$$\tilde{f}_n(x, t) = \frac{1}{\sqrt{2^n n!}} \left( \frac{\tilde{\epsilon}}{\pi} \right)^{1/4} H_n(\sqrt{\tilde{\epsilon}} x) \text{Exp} \left[ -\frac{\tilde{\epsilon}}{2} x^2 + i\tilde{a}_2 x^2 \right] \quad (4.12)$$

where  $\tilde{\epsilon} = 2\sqrt{(\tilde{a}_1 + \tilde{a}_3)^2 - \tilde{a}_2^2}$ . Then one can find the Schmidt decomposition of  $\psi_{0,0}(x_1, x_2 : t)$ , which is

$$\psi_{0,0}(x_1, x_2 : t) = \sum_n \sqrt{p_n} \left[ f_n(x_1, t) e^{-in\theta/2} e^{-i(E_0\tau_1 - \varphi/4)} \right] \left[ \tilde{f}_n(x_2, t) e^{-in\theta/2} e^{-i(E_0\tau_2 - \varphi/4)} \right] \quad (4.13)$$

where

$$\theta = \tan^{-1} \left( \frac{Z_2}{Z_1} \right) \quad \varphi = \tan^{-1} \left( \frac{(\kappa - 1)Z_1 Z_2}{Z_1^2 + \kappa Z_2^2} \right). \quad (4.14)$$

In Eq. (4.14)  $Z_1$ ,  $Z_2$ , and  $\kappa$  are given by

$$\kappa = \left[ 1 + \frac{\sin^2 \alpha \cos^2 \alpha}{\omega'_1 \omega'_2} \left\{ (\omega'_1 - \omega'_2)^2 + \left( \frac{\dot{b}_1}{b_1} - \frac{\dot{b}_2}{b_2} \right)^2 \right\} \right]^{1/2} \quad (4.15)$$

$$Z_1 = \omega'_1 - \omega'_2 \quad Z_2 = \frac{1}{\kappa} \left( \frac{\dot{b}_1}{b_1} - \frac{\dot{b}_2}{b_2} \right).$$

If  $\tilde{\omega}_j$  are time independent,  $Z_2$  becomes zero, which results in  $\theta = \varphi = 0$ . From the Schmidt decomposition one can define other bipartite entanglement measures such as Stückelberg entropy and the Schmidt basis is convenient to discuss on the entanglement in quantum optics, atom-field interaction, and electron-electron correlation[37, 38]. In this paper, however, we consider only Rényi and von Neumann entropies as bipartite entanglement measures.

## V. UNCERTAINTY

In order to discuss on the time-dependence of the uncertainty it is convenient to compute the Wigner function defined

$$W(x_1, x_2 : p_1, p_2 : t) \equiv \frac{1}{\pi^2} \int dy_1 dy_2 e^{-2i(p_1 y_1 + p_2 y_2)} \Psi^*(x_1 + y_1, x_2 + y_2 : t) \Psi(x_1 - y_1, x_2 - y_2 : t). \quad (5.1)$$

If we choose the wave function as  $\psi_{0,0}(x_1, x_2 : t)$ , the Wigner function becomes

$$W_{(0,0)}(x_1, x_2 : p_1, p_2 : t) = \frac{1}{\pi^2} \text{Exp} \left[ -A_1 x_1^2 - A_2 x_2^2 - B_1 p_1^2 - B_2 p_2^2 \right. \\ \left. + 2A_3 x_1 x_2 + 2B_3 p_1 p_2 + 2F(x_1 p_2 + x_2 p_1) + 2D_{11} x_1 p_1 + 2D_{22} x_2 p_2 \right] \quad (5.2)$$



where

$$\begin{aligned}
A_1 &= \frac{1}{\omega'_1 \omega'_2} \left[ \omega'_1 \omega'_2 \tilde{D} + \omega'_2 \left( \frac{\dot{b}_1}{b_1} \right)^2 \cos^2 \alpha + \omega'_1 \left( \frac{\dot{b}_2}{b_2} \right)^2 \sin^2 \alpha \right] \\
A_2 &= \frac{1}{\omega'_1 \omega'_2} \left[ \omega'_1 \omega'_2 D + \omega'_2 \left( \frac{\dot{b}_1}{b_1} \right)^2 \sin^2 \alpha + \omega'_1 \left( \frac{\dot{b}_2}{b_2} \right)^2 \cos^2 \alpha \right] \\
A_3 &= \frac{\sin \alpha \cos \alpha}{\omega'_1 \omega'_2} \left[ \omega'_1 \omega'_2 (\omega'_1 - \omega'_2) + \omega'_2 \left( \frac{\dot{b}_1}{b_1} \right)^2 - \omega'_1 \left( \frac{\dot{b}_2}{b_2} \right)^2 \right] \\
B_1 &= \frac{D}{\omega'_1 \omega'_2} \quad B_2 = \frac{\tilde{D}}{\omega'_1 \omega'_2} \quad B_3 = -\frac{\sin \alpha \cos \alpha}{\omega'_1 \omega'_2} (\omega'_1 - \omega'_2) \\
F &= \frac{\sin \alpha \cos \alpha}{\omega'_1 \omega'_2} \left( \omega'_2 \frac{\dot{b}_1}{b_1} - \omega'_1 \frac{\dot{b}_2}{b_2} \right) \quad D_{11} = -\frac{1}{\omega'_1 \omega'_2} \left( \omega'_2 \frac{\dot{b}_1}{b_1} \cos^2 \alpha + \omega'_1 \frac{\dot{b}_2}{b_2} \sin^2 \alpha \right) \\
D_{22} &= -\frac{1}{\omega'_1 \omega'_2} \left( \omega'_2 \frac{\dot{b}_1}{b_1} \sin^2 \alpha + \omega'_1 \frac{\dot{b}_2}{b_2} \cos^2 \alpha \right).
\end{aligned} \tag{5.3}$$

The Wigner function  $W_{(0,0)}(x_1, p_1 : t)$  is defined as

$$W_{(0,0)}(x_1, p_1 : t) = \int dx_2 dp_2 W_{(0,0)}(x_1, x_2 : p_1, p_2 : t). \tag{5.4}$$

Using Eq. (5.2) one can show

$$W_{(0,0)}(x_1, p_1 : t) = \frac{1}{\pi} \sqrt{\frac{\omega'_1 \omega'_2}{\bar{\eta}}} e^{-\alpha_1 x_1^2 - \alpha_2 p_1^2 + 2\alpha_3 x_1 p_1} \tag{5.5}$$

where

$$\begin{aligned}
\alpha_1 &= \frac{1}{\bar{\eta}} \left[ \tilde{D} \omega'_1 \omega'_2 + \omega'_2 \left( \frac{\dot{b}_1}{b_1} \right)^2 \cos^2 \alpha + \omega'_1 \left( \frac{\dot{b}_2}{b_2} \right)^2 \sin^2 \alpha \right] \\
\alpha_2 &= \frac{D}{\bar{\eta}} \quad \alpha_3 = -\frac{1}{\bar{\eta}} \left( \omega'_2 \frac{\dot{b}_1}{b_1} \cos^2 \alpha + \omega'_1 \frac{\dot{b}_2}{b_2} \sin^2 \alpha \right).
\end{aligned} \tag{5.6}$$

It is worthwhile noting that  $\alpha_j$  ( $j = 1, 2, 3$ ) satisfy

$$\alpha_1 \alpha_2 - \alpha_3^2 = \frac{\omega'_1 \omega'_2}{\bar{\eta}}.$$

One can show straightforwardly

$$\begin{aligned}
\int dx_1 dp_1 W_{(0,0)}(x_1, p_1 : t) &= 1 = \text{Tr} [\rho_{(0,0)}^A] \\
2\pi \int dx_1 dp_1 W_{(0,0)}^2(x_1, p_1 : t) &= \sqrt{\frac{\omega'_1 \omega'_2}{\bar{\eta}}} = \text{Tr} [(\rho_{(0,0)}^A)^2].
\end{aligned} \tag{5.7}$$

In terms of the Wigner function the average of a quantity  $\mathcal{O}(x_1, p_1)$  is defined as

$$\langle \mathcal{O} \rangle (x_1, p_1) \equiv \int \mathcal{O}(x_1, p_1) W_{(0,0)}(x_1, p_1) dx_1 dp_1. \quad (5.8)$$

Then it is straightforward to show that  $\langle x_1 \rangle = \langle p_1 \rangle = 0$  and

$$\langle x_1^2 \rangle = \frac{D}{2\omega'_1\omega'_2} \quad \langle p_1^2 \rangle = \frac{1}{2} \left[ \tilde{D} + \frac{1}{\omega'_1} \left( \frac{\dot{b}_1}{b_1} \right)^2 \cos^2 \alpha + \frac{1}{\omega'_2} \left( \frac{\dot{b}_2}{b_2} \right)^2 \sin^2 \alpha \right]. \quad (5.9)$$

Thus, the position-momentum uncertainty for the vacuum state becomes

$$(\Delta x_1 \Delta p_1)^2 = \frac{1}{4} \Omega(t) \quad (5.10)$$

where

$$\Omega(t) = \left( \frac{1}{\omega'_1} \cos^2 \alpha + \frac{1}{\omega'_2} \sin^2 \alpha \right) \left[ \left\{ \omega'_1 + \frac{1}{\omega'_1} \left( \frac{\dot{b}_1}{b_1} \right)^2 \right\} \cos^2 \alpha + \left\{ \omega'_2 + \frac{1}{\omega'_2} \left( \frac{\dot{b}_2}{b_2} \right)^2 \right\} \sin^2 \alpha \right]. \quad (5.11)$$

Using Eq. (4.10) one can compute also the uncertainty between  $x_2$  and  $p_2$ , In this case the uncertainty becomes  $(\Delta x_2 \Delta p_2)^2 = \tilde{\Omega}(t)/4$ , where

$$\tilde{\Omega}(t) = \left( \frac{1}{\omega'_1} \sin^2 \alpha + \frac{1}{\omega'_2} \cos^2 \alpha \right) \left[ \left\{ \omega'_1 + \frac{1}{\omega'_1} \left( \frac{\dot{b}_1}{b_1} \right)^2 \right\} \sin^2 \alpha + \left\{ \omega'_2 + \frac{1}{\omega'_2} \left( \frac{\dot{b}_2}{b_2} \right)^2 \right\} \cos^2 \alpha \right]. \quad (5.12)$$

If  $\tilde{\omega}_j$  are time-independent, both  $\Omega$  and  $\tilde{\Omega}$  reduces to  $1 + \frac{(\omega'_1 - \omega'_2)^2}{\omega'_1 \omega'_2} \sin^2 \alpha \cos^2 \alpha$ . Thus minimum uncertainty occurs at  $\alpha = 0$  while maximum uncertainty occurs at  $\alpha = \pm\pi/4$ .

## VI. THREE MODELS

In this section we consider the dynamics of entanglement and uncertainty in the three models. First two models are toy models, which are introduced to examine the effect of time-dependence of the angular frequencies and rotation angle  $\alpha$  in the dynamics. In third model we consider more realistic quenched model, where the dynamics can be solved analytically. Although we can consider the general case by solving the Ermakov equation (3.4) numerically, this fully general model is not considered in this paper because we would like to confine ourselves to the analytic cases.

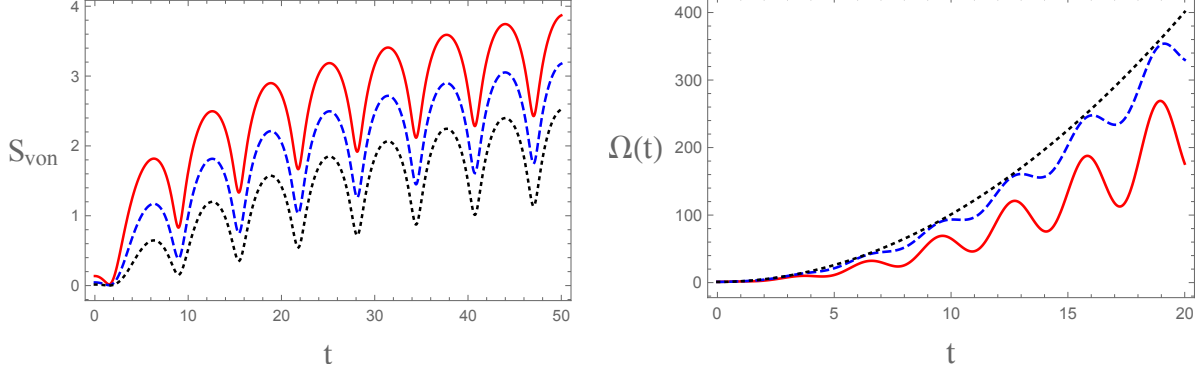


FIG. 1: (Color online) The time-dependence of von Neumann entropy (Fig. 1(a)) and uncertainty  $\Omega(t)$  (Fig. 1(b)) when  $\omega_{1,i} = 1$ ,  $\omega_{1,f} = 0$ ,  $\omega_{2,i} = 2$ , and  $\omega_{2,f} = 0.5$  for various  $\alpha$ . (a) Dynamics of von Neumann entropy for  $\alpha = \pi/4$  (red solid line),  $\alpha = \pi/12$  (blue dashed line), and  $\alpha = \pi/24$  (black dotted line). (b) Dynamics of uncertainty for  $\alpha = \pi/4$  (red solid line),  $\alpha = \pi/8$  (blue dashed line), and  $\alpha = 0$  (black dotted line).

The first model we consider is a simple case that one of angular frequency in  $\tilde{\omega}_j$  is zero at late time. We choose

$$\tilde{\omega}_1(t) = \begin{cases} \omega_{1,i} & t = 0 \\ \omega_{1,f} = 0 & t > 0 \end{cases} \quad \tilde{\omega}_2(t) = \begin{cases} \omega_{2,i} & t = 0 \\ \omega_{2,f} & t > 0. \end{cases} \quad (6.1)$$

From Eq. (2.5) this is achieved by  $\omega_1\omega_2 = \pm J$  with  $\omega_2^2 > \omega_1^2$  at  $t > 0$ . In this case  $b_1(t)$  and  $b_2(t)$  become

$$b_1(t) = \sqrt{1 + \omega_{1,i}^2 t^2} \quad b_2(t) = \sqrt{\left(\frac{\omega_{2,f}^2 - \omega_{2,i}^2}{2\omega_{2,f}^2}\right) \cos(2\omega_{2,f}t) + \left(\frac{\omega_{2,f}^2 + \omega_{2,i}^2}{2\omega_{2,f}^2}\right)}. \quad (6.2)$$

The time-dependence of the von Neumann entropy for  $\alpha = \pi/4$  (red solid line),  $\alpha = \pi/12$  (blue dashed line), and  $\alpha = \pi/24$  (black dotted line) is plotted in Fig. 1(a) when  $\omega_{1,i} = 1$ ,  $\omega_{1,f} = 0$ ,  $\omega_{2,i} = 2$ , and  $\omega_{2,f} = 0.5$ . It exhibits an increasing behavior with oscillation. This oscillation is mainly due to  $b_2(t)$ . The figure shows that the coupled harmonic oscillator is more entangled with increasing  $|\alpha|$ . This can be expected from the fact that the oscillator becomes separable when  $\alpha = 0$ . The time-dependence of uncertainty  $\Omega(t) = (2\Delta x_1 \Delta p_1)^2$  is plotted in Fig. 1(b) for  $\alpha = \pi/4$  (red solid line),  $\alpha = \pi/8$  (blue dashed line) and  $\alpha = 0$  (black dotted line). The uncertainty is maximized at the separable oscillator system and is minimized at  $|\alpha| = \pi/4$  at most domain of time. However, this order is reversed at the

small  $t$  region (for our case  $0 < t < 0.773$ ). In this region the uncertainty is maximized at  $\alpha = \pi/4$  and is minimized at  $\alpha = 0$ . The oscillatory behavior is also due to  $b_2(t)$ .

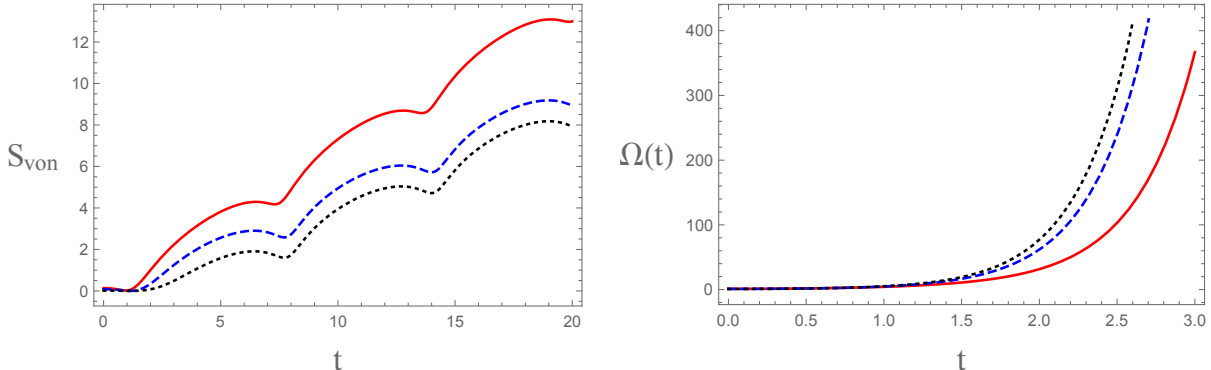


FIG. 2: (Color online) The time-dependence of von Neumann entropy (Fig. 2(a)) and uncertainty  $\Omega(t)$  (Fig. 2(b)) when  $\omega_{1,i} = 1$ ,  $\omega_{1,f} = 0.7$ ,  $\omega_{2,i} = 2$ , and  $\omega_{2,f} = 0.5$  for various  $\alpha$ . (a) Dynamics of von Neumann entropy for  $\alpha = \pi/4$  (red solid line),  $\alpha = \pi/8$  (blue dashed line), and  $\alpha = \pi/24$  (black dotted line). (b) Dynamics of uncertainty for  $\alpha = \pi/4$  (red solid line),  $\alpha = \pi/8$  (blue dashed line), and  $\alpha = 0$  (black dotted line).

Second simple model we consider is a case that one of angular frequency in  $\tilde{\omega}_j$  is imaginary at late time. We choose

$$\tilde{\omega}_1(t) = \begin{cases} \omega_{1,i} & t = 0 \\ i\omega_{1,f} & t > 0 \end{cases} \quad \tilde{\omega}_2(t) = \begin{cases} \omega_{2,i} & t = 0 \\ \omega_{2,f} & t > 0. \end{cases} \quad (6.3)$$

From Eq. (2.5) this is achieved by  $J^2 > \omega_1^2 \omega_2^2$  with  $\omega_2^2 > \omega_1^2$  at  $t > 0$ . In this case  $b_2(t)$  is not changed and  $b_1(t)$  becomes

$$b_1(t) = \sqrt{\left( \frac{\omega_{1,f}^2 + \omega_{1,i}^2}{2\omega_{1,f}^2} \right) \cosh(2\omega_{1,f}t) + \left( \frac{\omega_{1,f}^2 - \omega_{1,i}^2}{2\omega_{1,f}^2} \right)}. \quad (6.4)$$

The time-dependence of the von Neumann entropy for  $\alpha = \pi/4$  (red solid line),  $\alpha = \pi/8$  (blue dashed line), and  $\alpha = \pi/24$  (black dotted line) is plotted in Fig. 2(a) when  $\omega_{1,i} = 1$ ,  $\omega_{1,f} = 0.7$ ,  $\omega_{2,i} = 2$ , and  $\omega_{2,f} = 0.5$ . Like a previous case it exhibits an increasing behavior with oscillation. The difference is the fact that the von Neumann entropy in the present case is rapidly increasing in time compared to the previous case. This seems to be mainly due to exponential behavior of  $b_1(t)$  in time. The time-dependence of uncertainty  $\Omega(t) =$

$(2\Delta x_1 \Delta p_1)^2$  is plotted in Fig. 2(b) for  $\alpha = \pi/4$  (red solid line),  $\alpha = \pi/8$  (blue dashed line) and  $\alpha = 0$  (black dotted line). Although whole behavior is similar to the previous case, the oscillatory behavior disappears in this case. This is due to the rapid increasing behavior of  $\Omega(t)$ , thus the amplitude of oscillation is negligible. In this case also the order of uncertainty is reversed at the small  $t$  region (for this case  $t \leq t \leq 0.713$ ).

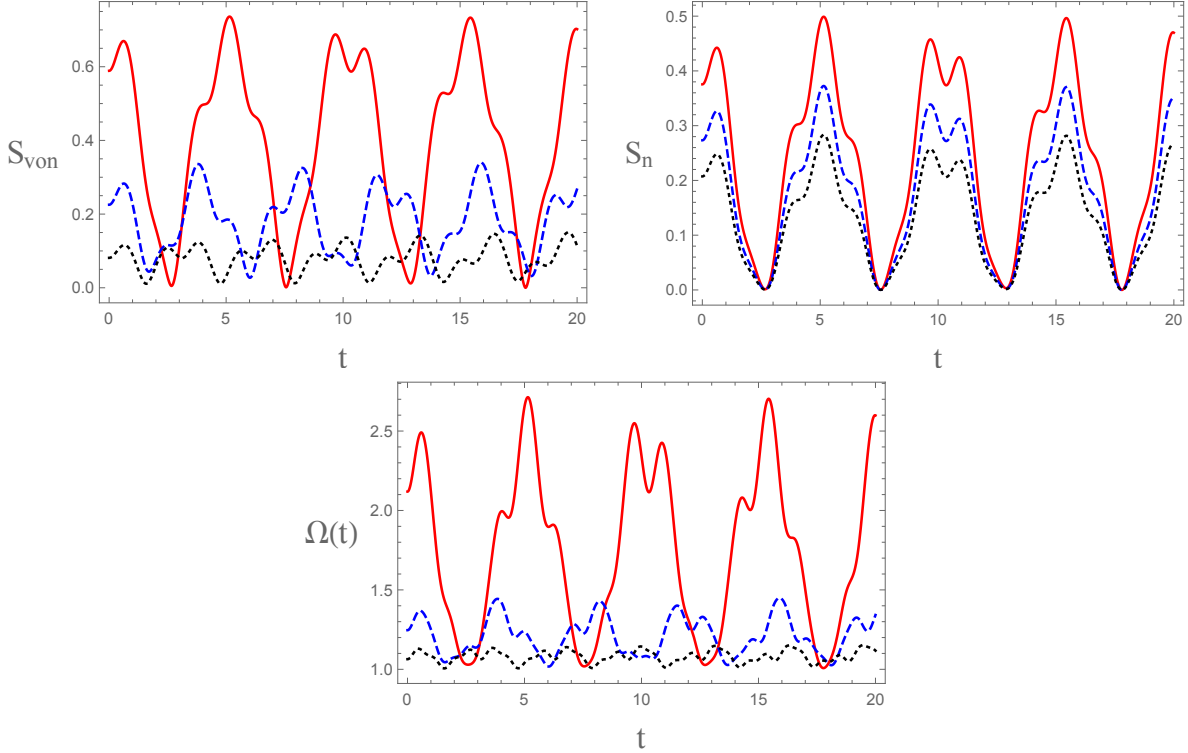


FIG. 3: (Color online) The time-dependence of von Neumann entropy (Fig. 3(a)), Rényi entropy  $S_n$  (Fig. 3(b)), and uncertainty  $\Omega(t)$  (Fig. 3(c)) when  $\omega_{1,i} = 1$ ,  $\omega_{1,f} = 1.3$ ,  $\omega_{2,i} = 1.5$ , and  $\omega_{2,f} = 1.8$  for various  $J$ . (a) Dynamics of von Neumann entropy for  $J = 1.1$  (red solid line),  $J = 0.9$  (blue dashed line), and  $J = 0.6$  (black dotted line). (b) Dynamics of Rényi entropy for  $n = 2$  (red solid line),  $n = 4$  (blue dashed line), and  $n = 100$  (black dotted line). In this figure  $J$  is fixed as 1.1. (c) Dynamics of uncertainty for  $J = 1.1$  (red solid line),  $J = 0.9$  (blue dashed line), and  $J = 0.6$  (black dotted line).

The final and more realistic model we consider is a quenched model. In this model we choose the original angular frequencies  $\omega_j$  as

$$\omega_1(t) = \begin{cases} \omega_{1,i} & t = 0 \\ \omega_{1,f} & t > 0 \end{cases} \quad \omega_2(t) = \begin{cases} \omega_{2,i} & t = 0 \\ \omega_{2,f} & t > 0. \end{cases} \quad (6.5)$$

In this case the rotation angle  $\alpha$  is completely determined by Eq. (2.3) if  $J$  is given. Also  $\tilde{\omega}_{1,i}$ ,  $\tilde{\omega}_{1,f}$ ,  $\tilde{\omega}_{2,i}$ , and  $\tilde{\omega}_{2,f}$  are completely determined by Eq. (2.5). The scale factor  $b_j(t)$  become

$$b_j(t) = \sqrt{\left(\frac{\tilde{\omega}_{j,f}^2 - \tilde{\omega}_{j,i}^2}{2\tilde{\omega}_{j,f}^2}\right) \cos(2\tilde{\omega}_{j,f}t) + \left(\frac{\tilde{\omega}_{j,f}^2 + \tilde{\omega}_{j,i}^2}{2\tilde{\omega}_{j,f}^2}\right)} \quad (j = 1, 2). \quad (6.6)$$

The time-dependence of the von Neumann entropy  $S_{von}$ , Rényi entropy  $S_n$ , and uncertainty  $\Omega(t)$  is plotted in Fig. 3 when  $\omega_{1,i} = 1$ ,  $\omega_{1,f} = 1.3$ ,  $\omega_{2,i} = 1.5$ , and  $\omega_{2,f} = 1.8$  with varying  $J$  (Fig. 3(a), Fig. 3(c)) or  $n$  (Fig. 3(b)). In Fig. 3(a) the von Neumann entropy is plotted for  $J = 1.1$  (red solid line),  $J = 0.9$  (blue dashed line), and  $J = 0.6$  (black dotted line). Unlike the previous toy models the large  $\alpha$  (or large  $J$ ) does not guarantees higher entanglement in the full range of time in this realistic model. Another difference is a fact that the time-dependence of the von Neumann entropy exhibits a double oscillatory behavior. This is due to the fact that the trigonometric function is involved in both  $b_1(t)$  and  $b_2(t)$ . The time-dependence of the Rényi entropy is plotted for  $n = 2$  (red solid line),  $n = 4$  (blue dashed line), and  $n = 100$  (black dotted line). In this figure  $J$  is fixed as 1.1. It also exhibits a double oscillatory behavior. With increasing  $n$  the Rényi entropy decreases, and eventually approaches to  $S_\infty = -\ln(1 - \xi)$ . Most striking difference arises in the dynamics of the uncertainty  $\Omega(t) = (2\Delta x_1 \Delta p_1)^2$ . This is plotted on Fig. 3(c) for  $J = 1.1$  (red solid line),  $J = 0.9$  (blue dashed line), and  $J = 0.6$  (black dotted line). In the previous toy models large  $\alpha$  yields small  $\Omega(t)$  at large time region. However this does not hold in this realistic model. In this model large  $J$  yields large  $\Omega(t)$  in most region of time domain. The surprising fact is that  $S_{von}$  and  $\Omega$  exhibit similar pattern. We do not know whether or not this is universal property. If so, one can use the uncertainty as a candidate of entanglement measure after rescaling it appropriately. It also exhibits a double oscillatory behavior due to the scale factors  $b_j(t)$ .

## VII. CONCLUSIONS

The dynamics of the entanglement and uncertainty relation is examined by solving the TDSE of the coupled harmonic oscillator system when the angular frequencies  $\omega_j$  and coupling constant  $J$  are arbitrarily time-dependent and two oscillators are in ground states initially. To show the dynamics pictorially we introduce two toy models and one realistic

quenched model. While the dynamics can be conjectured by simple consideration in the toy models, the dynamics in the realistic quenched model is somewhat different from those in the toy models. In particular, the dynamics of entanglement exhibits similar behavior to dynamics of uncertainty parameter in the realistic quenched model. We do not know whether or not this is general feature.

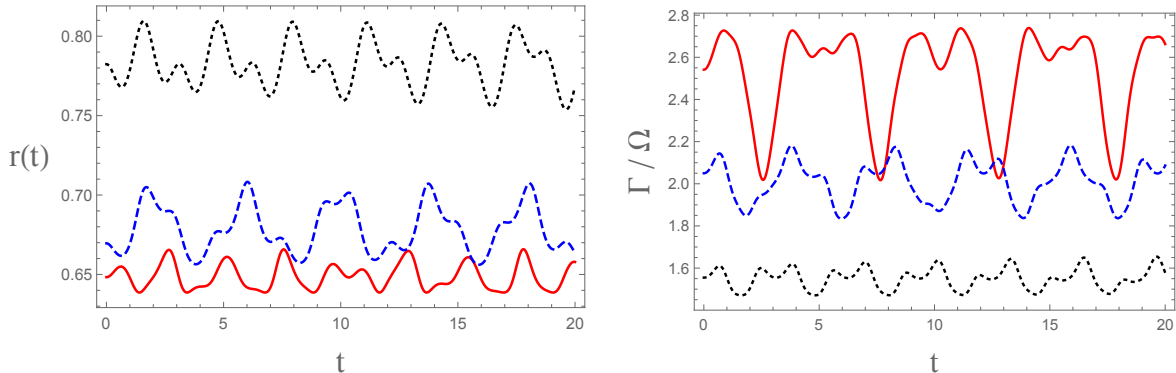


FIG. 4: (Color online) The time-dependence of ratio for mixedness  $r(t)$  (Fig. 4(a)) and uncertainties  $\Gamma(t)/\Omega(t)$  (Fig. 4(b)) between  $\rho_{(0,0)}^A$  and  $\rho_{(0,1)}^A$  in the realistic quenched model. We choose  $\omega_{1,i} = 1$ ,  $\omega_{1,f} = 1.3$ ,  $\omega_{2,i} = 1.5$ , and  $\omega_{2,f} = 1.8$  for  $J = 1.1$  (red solid line),  $J = 0.9$  (blue dashed line), and  $J = 0.6$  (black dotted line). Since  $r(t) < 1$  in the full range of time, Fig. 4(a) indicates that  $\rho_{(0,1)}^A$  is more mixed state than  $\rho_{(0,0)}^A$ . It is of interest to note that  $\rho_{(0,1)}^A$  becomes more and more mixed compared to  $\rho_{(0,0)}^A$  with increasing the coupling constant  $J$ . Fig. 4(b) shows that the uncertainty  $\Delta x_1 \Delta p_1$  increases in  $\rho_{(0,1)}^A$  compared to that of  $\rho_{(0,0)}^A$ . The increasing rate becomes larger with increasing the coupling constant  $J$ .

It is natural to ask how the dynamics is changed when initial condition is changed. If, for example, two oscillators are in ground and first-excited states initially, the reduced density matrix becomes

$$\rho_{(0,1)}^A(x_1, x_1' : t) = 2\omega_2' \rho_{(0,0)}^A(x_1, x_1' : t) \left[ \frac{\cos^2 \alpha}{2D} + F_1 x_1^2 + F_1^* x_1'^2 + F_2 x_1 x_1' \right] \quad (7.1)$$

where  $\rho_{(0,0)}^A(x_1, x'_1 : t)$  is given in Eq. (4.2) and

$$F_1 = \frac{\sin^2 \alpha \cos^2 \alpha}{4D^2} \left[ (\omega'_1 - \omega'_2) \{ \omega'_1 (1 + \sin^2 \alpha) + \omega'_2 \cos^2 \alpha \} \right. \\ \left. - \cos^2 \alpha \left( \frac{\dot{b}_1}{b_1} - \frac{\dot{b}_2}{b_2} \right)^2 - 2i\omega'_1 \left( \frac{\dot{b}_1}{b_1} - \frac{\dot{b}_2}{b_2} \right) \right] \quad (7.2)$$

$$F_2 = \frac{1}{D} (2a_3 \cos^2 \alpha + \omega'_1 \sin^2 \alpha).$$

The explicit expression of  $a_3$  is given in Eq. (4.3). Then one can show

$$\text{Tr} [\rho_{(0,1)}^A] \equiv \int dx \rho_{(0,1)}^A(x, x : t) = 1 \quad (7.3)$$

$$\text{Tr} [(\rho_{(0,1)}^A)^2] \equiv \int dx dx' \rho_{(0,1)}^A(x, x' : t) \rho_{(0,1)}^A(x', x : t) = \text{Tr} [(\rho_{(0,0)}^A)^2] r(t)$$

where  $r(t)$  is ratio of mixedness between  $\rho_{(0,0)}^A$  and  $\rho_{(0,1)}^A$  and its explicit expression is

$$r(t) = 4\omega_2'^2 \left[ \frac{\cos^4 \alpha}{4D^2} + \frac{\cos^2 \alpha}{4Da_1(a_1 + 2a_3)} \{ (F_1 + F_1^*)a_1 + (F_1 + F_1^* + F_2)a_3 \} \right. \quad (7.4)$$

$$+ \frac{1}{16a_1^2(a_1 + 2a_3)^2} \left[ a_1^2 \{ (F_1 + F_1^*)^2 + 4|F_1|^2 + F_2^2 \} + a_3^2 \{ 3(F_1 + F_1^*)^2 + 3F_2(2F_1 + 2F_1^* + F_2) \} \right. \\ \left. \left. + 2a_1a_3 \{ (F_1 + F_1^*)^2 + 4|F_1|^2 + F_2(3F_1 + 3F_1^* + F_2) \} \right] \right].$$

We expect that the entanglement between ground and first-excited harmonic oscillators is very small compared to that between two ground state harmonic oscillators. However, it is difficult to show this explicitly because the analytic derivation of eigenvalues and eigenfunctions for  $\rho_{(0,1)}^A(x, x' : t)$  does not seem to be simple matter, at lease for us. We hope to discuss the dynamics of entanglement for general excited  $(m, n)$  state in the future. The time-dependence of the uncertainty  $\Delta x_1 \Delta p_1$  for  $\rho_{(0,1)}^A$  can be computed analytically. The Wigner function  $W_{(0,1)}(x_1, p_1, t)$  for this state becomes

$$W_{(0,1)}(x_1, p_1, t) = W_{(0,0)}(x_1, p_1, t) [h_0(t) + h_1(t)x_1^2 + h_2(t)p_1^2 + 2h_3(t)x_1p_1] \quad (7.5)$$



where  $W_{(0,0)}(x_1, p_1, t)$  is the Wigner function for  $\psi_{0,0}(x_1, x_2, t)$  given in Eq. (5.5) and

$$\begin{aligned}
h_0(t) &= \frac{\omega'_1 \omega'_2}{\bar{\eta}} \cos 2\alpha \tag{7.6} \\
h_1(t) &= \frac{2\omega'_2 \sin^2 \alpha}{\bar{\eta}^2} \left\{ \left[ \omega'_1 \tilde{D} + \cos^2 \alpha \frac{\dot{b}_1}{b_1} \left( \frac{\dot{b}_1}{b_1} - \frac{\dot{b}_2}{b_2} \right) \right]^2 + \left[ \omega'_1 \frac{\dot{b}_2}{b_2} \sin^2 \alpha + \omega'_2 \frac{\dot{b}_1}{b_1} \cos^2 \alpha \right]^2 \right\} \\
h_2(t) &= \frac{2\omega'_2 \sin^2 \alpha}{\bar{\eta}^2} \left[ D^2 + \cos^4 \alpha \left( \frac{\dot{b}_1}{b_1} - \frac{\dot{b}_2}{b_2} \right)^2 \right] \\
h_3(t) &= \frac{2\omega'_2 \sin^2 \alpha}{\bar{\eta}^2} \left\{ \cos^2 \alpha \left( \frac{\dot{b}_1}{b_1} - \frac{\dot{b}_2}{b_2} \right) \left[ \omega'_1 \tilde{D} + \cos^2 \alpha \frac{\dot{b}_1}{b_1} \left( \frac{\dot{b}_1}{b_1} - \frac{\dot{b}_2}{b_2} \right) \right] \right. \\
&\quad \left. + D \left[ \omega'_1 \frac{\dot{b}_2}{b_2} \sin^2 \alpha + \omega'_2 \frac{\dot{b}_1}{b_1} \cos^2 \alpha \right] \right\}.
\end{aligned}$$

Then it is straight to show that the uncertainty relation for  $\rho_{(0,1)}^A$  becomes  $(\Delta x_1 \Delta p_1)^2 = \Gamma(t)/4$ , where

$$\begin{aligned}
\Gamma(t) &= \left( \frac{\bar{\eta}}{\omega'_1 \omega'_2} \right)^2 \left[ \left( h_0 \alpha_2 + \frac{h_2}{2} \right) + \frac{3\bar{\eta}}{2\omega'_1 \omega'_2} (h_1 \alpha_2^2 + h_2 \alpha_3^2 + 2h_3 \alpha_2 \alpha_3) \right] \tag{7.7} \\
&\quad \times \left[ \left( h_0 \alpha_1 + \frac{h_1}{2} \right) + \frac{3\bar{\eta}}{2\omega'_1 \omega'_2} (h_2 \alpha_1^2 + h_1 \alpha_3^2 + 2h_3 \alpha_1 \alpha_3) \right]
\end{aligned}$$

where  $\alpha_j$  are defined in Eq. (5.6).

The time-dependence of the ratios  $r(t)$  and  $\Gamma(t)/\Omega(t)$  for the realistic quenched model is plotted in Fig. 4, where  $\omega_{1,i} = 1$ ,  $\omega_{1,f} = 1.3$ ,  $\omega_{2,i} = 1.5$ , and  $\omega_{2,f} = 1.8$  are chosen. The red solid, blue dashed, and black dotted lines are correspondent with  $J = 1.1$ ,  $J = 0.9$ , and  $J = 0.6$  respectively. The fact  $r(t) < 1$  in the full range of time indicates that  $\rho_{(0,1)}^A$  is more mixed than  $\rho_{(0,0)}^A$ . It is of interest to note that  $\rho_{(0,1)}^A$  becomes more mixed compared to  $\rho_{(0,0)}^A$  with increasing the coupling constant  $J$ . Fig. 4(b) indicates that the uncertainty  $\Delta x_1 \Delta p_1$  increases in  $\rho_{(0,1)}^A$  compared to that of  $\rho_{(0,0)}^A$ . The increasing rate becomes larger with increasing the coupling constant  $J$ .

Another interesting issue related to the entanglement of the coupled harmonic oscillators is multipartite entanglement. Consider the three coupled harmonic oscillator system, whose Hamiltonian is

$$H = \frac{1}{2}(p_1^2 + p_2^2 + p_3^2) + \frac{1}{2}(\omega_1^2(t)x_1^2 + \omega_2^2(t)x_2^2 + \omega_3^2(t)x_3^2) - (J_{12}(t)x_1x_2 + J_{13}(t)x_1x_3 + J_{23}(t)x_2x_3). \tag{7.8}$$

We conjecture that the TDSE of this system can be solved analytically. However, computation of the tripartite entanglement seems to be a formidable task. First of all we do not know what kind of entanglement measure can be computed. In a qubit system we usually use the three-tangle[39] or  $\pi$ -tangle[40] to measure the tripartite entanglement. However, it is not clear whether these tangles can be computed analytically in the coupled harmonic oscillator system or not. We hope to visit this issue in the future.

**Acknowledgement:** This work was supported by the Kyungnam University Foundation Grant, 2016.

- 
- [1] E. Schrödinger, *Die gegenwärtige Situation in der Quantenmechanik*, *Naturwissenschaften*, **23** (1935) 807.
  - [2] M. A. Nielsen and I. L. Chuang, *Quantum Computation and Quantum Information* (Cambridge University Press, Cambridge, England, 2000).
  - [3] R. Horodecki, P. Horodecki, M. Horodecki, and K. Horodecki, *Quantum Entanglement*, *Rev. Mod. Phys.* **81** (2009) 865 [quant-ph/0702225] and references therein.
  - [4] A. Einstein, B. Podolsky and N. Rosen, *Can quantum-mechanical description of physical reality be considered complete?*, *Phys. Rev.* **A47** (1935) 777.
  - [5] C. H. Bennett, G. Brassard, C. Crépeau, R. Jozsa, A. Peres and W. K. Wootters, *Teleporting an Unknown Quantum State via Dual Classical and Einstein-Podolsky-Rosen Channels*, *Phys. Rev. Lett.* **70** (1993) 1895.
  - [6] C. H. Bennett and S. J. Wiesner, *Communication via one- and two-particle operators on Einstein-Podolsky-Rosen states*, *Phys. Rev. Lett.* **69** (1992) 2881.
  - [7] V. Scarani, S. L. Braunstein, N. Gisin and A. Acín, *Quantum cloning*, *Rev. Mod. Phys.* **77** (2005) 1225 [quant-ph/0511088] and references therein.
  - [8] A. K. Ekert, *Quantum Cryptography Based on Bell's Theorem*, *Phys. Rev. Lett.* **67** (1991) 661.
  - [9] C. Kollmitzer and M. Pivk, *Applied Quantum Cryptography* (Springer, Heidelberg, Germany, 2010).
  - [10] T. D. Ladd, F. Jelezko, R. Laflamme, Y. Nakamura, C. Monroe, and J. L. O'Brien, *Quantum Computers*, *Nature*, **464** (2010) 45 [arXiv:1009.2267 (quant-ph)].

- [11] G. Vidal, *Efficient classical simulation of slightly entangled quantum computations*, Phys. Rev. Lett. **91** (2003) 147902 [quant-ph/0301063].
- [12] S. Ghernaouti-Helie, I. Tashi, T. Laenger, and C. Monyk, *SECOQC Business White Paper*, arXiv:0904.4073 (quant-ph).
- [13] S. Hill and W. K. Wootters, *Entanglement of a Pair of Quantum Bits*, Phys. Rev. Lett. **78** (1997) 5022 [quant-ph/9703041]; W. K. Wootters, *Entanglement of Formation of an Arbitrary State of Two Qubits*, *ibid.* **80** (1998) 2245 [quant-ph/9709029].
- [14] R. Horodecki and M. Horodecki, *Information-theoretic aspects of inseparability of mixed states*, Phys. Rev. **A 54** (1996) 1838 [quant-ph/9607007].
- [15] J. D. Bekenstein, *Black Holes and Entropy*, Phys. Rev. **D 7** (1973) 2333.
- [16] S. W. Hawking, *Breakdown of predictability in gravitational collapse*, Phys. Rev. **D 14** (1976) 2460.
- [17] G. 't Hooft, *On the quantum structure of a black hole*, Nucl. Phys. **B 256** (1985) 727.
- [18] L. Bombelli, R. K. Koul, J. Lee, and R. D. Sorkin, *Quantum source of entropy for black holes*, Phys. Rev. **D 34** (1986) 373.
- [19] M. Srednicki, *Entropy and Area*, Phys. Rev. Lett. **71** (1993) 666.
- [20] S. N. Solodukhin, *Entanglement Entropy of Black Holes*, Living Rev. Relativity, **14** (2011) 8 [arXiv:1104.3712 (hep-th)].
- [21] J. Eisert, M. Cramer, and M. B. Plenio, *Area laws for the entanglement entropy - a review*, Rev. Mod. Phys. **82** (2010) 277 [arXiv:0808.3773 (quant-ph)].
- [22] G. Vidal, J. I. Latorre, E. Rico, and A. Kitaev, *Entanglement in Quantum Critical Phenomena*, Phys. Rev. Lett. **90** (2003) 227902 (quant-ph/0211074 ).
- [23] M. Levin and X.-G. Wen, *Detecting Topological Order in a Ground State Wave Function*, Phys. Rev. Lett. **96** (2006) 110405 [cond-mat/0510613 ].
- [24] H.-C. Jiang, Z. Wang, and L. Balents, *Identifying topological order by entanglement entropy*, Nat. Phys. **8** (2012) 902 [arXiv:1205.4289 (cond-mat)].
- [25] C. Cohen-Tannoudji, B. Diu, and F. Laloë, *Quantum Mechanics* (John Wiley and Sons, Toronto, ON, 1977).
- [26] D. Han, Y. S. Kim, and M. E. Noz, *Coupled Harmonic Oscillators and Feynman's Rest of the Universe*, cond-mat/9705029.
- [27] R. P. Feymann, *Statistical Mechanics* (Benjamin/Cummings, Reading, MA, 1972).

- [28] D. N. Makarov, *Coupled harmonic oscillators and their quantum entanglement*, arXiv:1710.01158 [quant-ph].
- [29] S. Ghosh, K. S. Gupta, S. C. L. Srivastava, *Entanglement dynamics following a sudden quench: an exact solution*, arXiv:1709.02202 [quant-ph].
- [30] S. Ikeda and F. Fillaux, *Incoherent elastic-neutron-scattering study of the vibrational dynamics and spin-related symmetry of protons in the  $KHCO_3$  crystal*, Phys. Rev. **B 59** (1999) 4134.
- [31] F. Fillaux, *Quantum entanglement and nonlocal proton transfer dynamics in dimers of formic acid and analogues*, Chem. Phys. Lett. **408** (2005) 302.
- [32] E. Romero, R. Augulis, V. I. Novoderezhkin, M. Ferretti, J. Thieme, D. Zigmantas, and R. van Grondelle, *Quantum coherence in photosynthesis for efficient solar-energy conversion*, Nat. Phys. **10** (2014) 676.
- [33] A. Halpin, P. J. M. Johnson, R. Tempelaar, R. S. Murphy, J. Knoester, T. L. C. Jansen, and R. J. D. Miller, *Two-dimensional spectroscopy of a molecular dimer unveils the effects of vibronic coupling on exciton coherences*, Nat. Chem. **6** (2014) 196.
- [34] H. R. Lewis Jr., and W. B. Riesenfeld, *An Exact Quantum Theory of the TimeDependent Harmonic Oscillator and of a Charged Particle in a TimeDependent Electromagnetic Field*, J. Math. Phys. **10** (1969) 1458.
- [35] M. A. Lohe, *Exact time dependence of solutions to the time-dependent Schrödinger equation*, J. Phys. A: Math. Theor. **42** (2009) 035307.
- [36] E. Pinney, *The nonlinear differential equation*, Proc. Amer. Math. Soc. **1** (1950) 681.
- [37] R. Grobe, K. Rzazewski and J. H. Eberly, *Measure of electron-electron correlation in atomic physics*, J. Phys. **B 27** (1994) L503.
- [38] A. Ekert and P. L. Knight, *Entangled quantum systems and the Schmidt decomposition*, Amer. J. Phys. **63** (1995) 415.
- [39] V. Coffman, J. Kundu and W. K. Wootters, *Distributed entanglement*, Phys. Rev. **A 61** (2000) 052306 [quant-ph/9907047].
- [40] Y. U. Ou and H. Fan, *Monogamy Inequality in terms of Negativity for Three-Qubit States*, Phys. Rev. **A75** (2007) 062308 [quant-ph/0702127].